Element-By-Element and Implicit-Explicit Finite Element Formulations for Computational Fluid Dynamics*

T. E. TEZDUYAR† AND J. LIOU†

Abstract. Element-by-element approximate factorization, implicit-explicit and adaptive implicit-explicit approximation procedures are presented for the finite element formulation of large-scale fluid dynamics problems. The element-by-element approximation scheme totally eliminates the need for formation, storage and inversion of large global matrices. Implicit-explicit schemes, which are approximations to implicit schemes, substantially reduce the computational burden associated with large global matrices. In the adaptive implicit-explicit scheme the implicit elements are selected adaptively based on element level stability and accuracy considerations. This scheme provides implicit refinement where it is needed.

The methods are applied to various problems governed by the convection-diffusion and incompressible Navier-Stokes equations. In all cases studied, the results obtained are indistinguishable from those obtained by the implicit formulations.

1. Introduction.

Significant improvements have been made in computer memory and speed in recent years. However, the existing computer power is still far behind the demands from scientists for large-scale fluid dynamics calculations. Implicit schemes, which are desirable for their stability and accuracy properties, lead to large global coefficient matrices which need to be fomed, stored and inverted. Direct management of such matrices is very difficult for large-scale, geometrically complicated two-dimensional problems and is virtually impossible for large-scale three-dimensional problems.

In this paper we present element-by-element (EBE) approximate factorization, implicit-explicit, and adaptive implicit-explicit (AIE) schemes for large-scale computations in fluid dynamics. Compared to implicit methods these schemes posses, to a great extent, similar desirable stability and accuracy properties, yet result in substantial reduction in computer memory and CPU time demands.

To overcome the shortage of computer power, many researchers have developed algorithms for large-scale problems. In their application of domain decomposition methods, Glowinski, Dinh and Periaux [1] sucessfully coupled the incompressible

* This research was sponsored by the NASA-Johnson Space Center under contract NAS-9-17380, by NSF grant MSM-8552479 and by the Laboratory of Enhanced Oil Recovery, University of Houston.

† Department of Mechanical Engineering, University of Houston, Houston, Texas 77004.

viscous flow and incompressible potential flow models employed in different subdomains. A conjugate gradient method, which is basically suitable for the symmetric and positive-definite systems, was employed to solve the variational problem. For the nonsymmetric and nonpositive-definite systems one has to find an appropriate preconditioner for each problem. It needs much sophisticated work [2-4]. A three-dimensional flow simulation with 128^3 was made by Rogallo [5] with alternating
direction method. A new class of algorithms in numerical linear algebra which take advantage of the parallel computation capabilities of modern computers also provides hope [6].

The EBE scheme is somehow related to domain decomposition [1,7] and alternating direction (or operator splitting) [8-11] schemes. These schemes, contrary to the EBE method, are based on global approximations. The EBE method was first proposed by Hughes, Levit and Winget [12,13] with applications to transient heat conduction, structural and solid mechanics problems. Preliminary application to fluid mechanics problems within the context of the compressible Euler equations were presented in Hughes, Levit, Winget and Tezduyar [14].

In this paper we present our EBE formulation for problems with nonsymmetric, nonpositive-definite spatial differential operators. Currently we focus on the convection-diffusion and incompressible Navier-Stokes equations. In the EBE formulation global coefficient matrices are approximated by sequential product of much simpler matrices which are based on the most natural unit in finite element method - the element level matrix. Every calculation is done at the element level. The method keeps the versatility of the finite element formulation in its easy adjustment to irregular meshes. Other advantages of the finite element method such as easy implementation of the boundary conditions and the source terms are also retained in the EBE formulation.

Our implicit-explicit approximation schemes for fluid dynamics problems are based on the work of Hughes and Liu [15,16] which was for solid mechanics and heat transfer applications. We consider problems governed by the convection-diffusion and incompressible Navier-Stokes equations. In this approach, for the elements which are designated to be implicit, the element level matrices are kept as they are, whereas for the explicit elements the element level matrices are approximated by a diagonal matrix. The implicit element-explicit element decision is based on the local stability criterion.

In the adaptive implicit-explicit (AIE) scheme the implicit element-explicit element decision is made dynamically. The stability and accuracy criteria applied to each element, based on the solution from the previous iteration or previous time step, determine whether an element needs to be implicit. In this approach we can adaptively have implicit refinement where it is needed for stability and accuracy. Compared to other adaptive schemes which are based on grid movement or element subdividing, the AIE approach involves minimal bookkeeping and no geometric constrains; therefore the method is very easy to implement.

In section 2 model problems are described and their spatial and temporal discretizations are given. The EBE, implicit-explicit, and AIE schemes are discussed in sections 3, 4 and 5 respectively. Numerical results are presented in section 6 and the conclusions are given in section 7.

2. Model Problems -- Spatial and Temporal Discretizations.

We consider model problems governed by the convection-diffusion equation and the vorticity-stream function form of the two-dimensional Navier-Stokes equations. A formal statement of the problem and the corresponding spatial discretization for both cases are given below.

convection-diffusion equation.

Time-dependent convection-diffusion of an unknown scalar function Φ is governed by the following set of differential equations, boundary conditions, and initial condition:

$$\Phi_{,t} + \mathbf{u}\cdot\nabla\Phi = \nabla\cdot(\boldsymbol{\kappa}\nabla\Phi) + f \qquad \text{on } \Omega\times]0,T[\qquad (2.1)$$

$$\Phi(\mathbf{x},t) = g(\mathbf{x},t) \qquad \forall\,\mathbf{x}\in\Gamma_g,\ t\in]0,T[\qquad (2.2)$$

$$\mathbf{n}\cdot\boldsymbol{\kappa}\nabla\Phi(\mathbf{x},t) = h(\mathbf{x},t) \qquad \forall\,\mathbf{x}\in\Gamma_h,\ t\in]0,T[\qquad (2.3)$$

$$\Phi(\mathbf{x},0) = \Phi_0(\mathbf{x}) \qquad \text{on } \Omega \qquad (2.4)$$

where Γ_g and Γ_h are the mutually exclusive but complementary subsets of the boundary Γ with Dirichelet and Neumann type boundary conditions respectively. The velocity field $\mathbf{u} = \mathbf{u}(\mathbf{x})$ is given and $\boldsymbol{\kappa}$ is the conductivity matrix. The source term is given as $f = f(\mathbf{x},t)$. The unit normal vector to the boundary is denoted by $\mathbf{n}$, whereas g, h and Φ_0 are prescribed functions.

Finite element spatial discretization of (2.1) - (2.4) leads to the following semi-discrete equations:

$$\tilde{\mathbf{M}}\,\dot{\Phi} + \tilde{\mathbf{C}}\,\Phi = \tilde{\mathbf{F}} \qquad (2.5)$$

$$\Phi(0) = \Phi_0 \qquad (2.6)$$

where $\tilde{\mathbf{M}}$, $\tilde{\mathbf{C}}$, and $\tilde{\mathbf{F}}$ are the "mass" matrix, "stiffness" matrix, and the generalized "force" vector, respectively; Φ and $\dot{\Phi}$ represent the dependent variable and its temporal derivative at the nodes. The information regarding the initial condition is contained in vector Φ_0.

<u>vorticity-stream function form of the two-dimensional Navier-Stokes equations</u>.

The field equations consist of a time-dependent transport equation for the unknown vorticity function ω and an equation which relates the unknown stream function Ψ to vorticity. They are given as follows:

$$\omega_{,t} + \mathbf{u}\cdot\nabla\omega = \nu\,\nabla^2\omega \qquad \text{on } \Omega\times]0,T[\qquad (2.7)$$

$$\nabla^2\Psi = -\omega \qquad \text{on } \Omega \qquad (2.8)$$

The velocity field $\mathbf{u}$, which is now an unknown, is related to the stream function by the following equations:

$$u_1 = \partial\Psi/\partial x_2 \qquad (2.9)$$

$$u_2 = -\partial\Psi/\partial x_1 \qquad (2.10)$$

and ν is the kinematic viscosity.

The boundary conditions for ω and Ψ are given below:

$$\omega(\mathbf{x},t) = \tilde{g}(\mathbf{x},t) \qquad \forall \mathbf{x} \in \Gamma_{\tilde{g}},\ t \in]0,T[\qquad (2.11)$$

$$\nu\, \mathbf{n} \cdot \nabla\omega(\mathbf{x},t) = \tilde{h}(\mathbf{x},t) \qquad \forall \mathbf{x} \in \Gamma_{\tilde{h}},\ t \in]0,T[\qquad (2.12)$$

$$\Psi(\mathbf{x},t) = g(\mathbf{x},t) \qquad \forall \mathbf{x} \in \Gamma_{g},\ t \in]0,T[\qquad (2.13)$$

$$\mathbf{n} \cdot \nabla\Psi(\mathbf{x},t) = h(\mathbf{x},t) \qquad \forall \mathbf{x} \in \Gamma_{h},\ t \in]0,T[\qquad (2.14)$$

where $\Gamma_{\tilde{g}}$ and $\Gamma_{\tilde{h}}$ are the subsets of the boundary Γ with Dirichelet and Neumann type boundary conditions for ω, whereas Γ_g and Γ_h are similar boundary subsets for Ψ. The initial condition for the vorticity is given as

$$\omega(\mathbf{x},0) = \omega_0 \qquad \text{on } \Omega \qquad (2.15)$$

Finite element spatial discretization of (2.7) - (2.15) leads to the following equations:

$$\tilde{\mathbf{M}}\,\dot{\boldsymbol{\omega}} + \tilde{\mathbf{C}}\,\boldsymbol{\omega} = \tilde{\mathbf{F}} \qquad (2.16)$$

$$\boldsymbol{\omega}(0) = \boldsymbol{\omega}_0 \qquad (2.17)$$

$$-\mathbf{M}\,\boldsymbol{\omega} + \mathbf{K}\,\boldsymbol{\Psi} = \mathbf{F} \qquad (2.18)$$

where $\tilde{\mathbf{M}}$, $\tilde{\mathbf{C}}$, $\tilde{\mathbf{F}}$, $\mathbf{M}$, $\mathbf{K}$, and $\mathbf{F}$ are the matrices and vectors resulting from the spatial discretization; $\boldsymbol{\omega}$, $\dot{\boldsymbol{\omega}}$, and $\boldsymbol{\Psi}$ represent the vorticity, its temporal derivative and the stream function at the nodes. The initial condition for ω is represented by ω_0.

Remarks:

1. A streamline-upwind/Petrov-Galerkin (SUPG) formulation is employed for the spatial discretization of the transport equations. The formulations are well-known for their robust and accurate performance for problems with nonsymmetric spatial operators. Several papers can be found in scientific literature on this type of schemes. We will only mention the one by Tezduyar and Ganjoo [17] for the readers' information. For the purpose of this paper we describe the SUPG scheme employed in terms of the weighting function basis $\tilde{N}_a$; that is:

$$\tilde{N}_a = N_a + C_{2\tau}\, h/2\, \mathbf{s} \cdot \nabla N_a \qquad (2.19)$$

or

$$\tilde{N}_a = N_a + \tau\, \mathbf{u}\cdot\nabla N_a \tag{2.20}$$

where the subscript "a" refers to an element node; N_a is the solution function basis, h is the "element length" in the direction of **u**, and **s** is the unit vector in **u** direction. $C_{2\tau}$ and τ are related by the following expression:

$$C_{2\tau} = \| \mathbf{u} \| 2\, \tau / h \tag{2.21}$$

Various choices for $C_{2\tau}$ have been investigated by Tezduyar and Ganjoo [17].

2. The difficulty associated with the lack of boundary conditions for vorticity and its normal derivative on the no-slip surfaces is tackled by a discrete Green's formula approach which will be described in a future paper by Tezduyar, Glowinski, and Glaisner.

<u>temporal discretization</u>.

Consider the following class of semi-discrete equation systems:

$$\mathbf{M}\,\mathbf{a} + \mathbf{C}\,\mathbf{v} = \mathbf{F} \tag{2.22}$$

$$\mathbf{v}(0) = \mathbf{v}_0 \tag{2.23}$$

where the vector **a** is the temporal derivative of the vector **v**. We employ a predictor/multi-corrector transient integration algorithm [18] to solve (2.22) - (2.23). The algorithm can be summerized as follows:

(1) given $\mathbf{v}_0$

$$\mathbf{M}\,\mathbf{a}_0 + \mathbf{C}\,\mathbf{v}_0 = \mathbf{F} \tag{2.24}$$

$n \rightarrow n+1$

(2) predictor stage

$$\mathbf{v}_{n+1}{}^0 = \mathbf{v}_n + (1-\alpha)\,\Delta t\, \mathbf{a}_n \tag{2.25}$$

$$\mathbf{a}_{n+1}{}^0 = \mathbf{0} \tag{2.26}$$

$i \rightarrow i+1$

(3) corrector stage

$$\mathbf{R}_{n+1}{}^i = \mathbf{F}_{n+1} - \mathbf{M}\,\mathbf{a}_{n+1}{}^i - \mathbf{C}\,\mathbf{v}_{n+1}{}^i \tag{2.27}$$

$$\mathbf{M}^*\,\Delta\mathbf{a}_{n+1}{}^i = \mathbf{R}_{n+1}{}^i \tag{2.28}$$

$$\mathbf{a}_{n+1}{}^{i+1} = \mathbf{a}_{n+1}{}^i + \Delta\mathbf{a}_{n+1}{}^i \tag{2.29}$$

$$\mathbf{v}_{n+1}{}^{i+1} = \mathbf{v}_{n+1}{}^i + \alpha\,\Delta t\,\Delta\mathbf{a}_{n+1}{}^i \tag{2.30}$$

where $\alpha \in [0,1]$ is a parameter which controls the stability and accuracy. A subscript denotes the time step and a superscript denotes the iteration step. Convergence is checkedby inspecting the norm of $\mathbf{R}_{n+1}^{i}$ and Δa_{n+1}^{i}.

Remarks:

1. A consistent derivation for $\mathbf{M}^*$ gives the following expression:

$$\mathbf{M}^* = \mathbf{M} + \alpha \Delta t \, \mathbf{C} \tag{2.31}$$

If left as it is, this expression for $\mathbf{M}^*$ leads to an implicit formulation which requires only one correction for linear systems. However, for nonlinear systems one needs to have as many corrections as the convergence criterion dictates.

2. A choice of

$$\mathbf{M}^* = \mathbf{M}_L \tag{2.32}$$

where $\mathbf{M}_L$ is a lumped version of matrix $\mathbf{M}$, leads to an explicit formulation. Explicit formulations in general are less stable, less accurate, but also less costly (less memory and less CPU time) compared to implicit schemes. The conditional stability of these methods are usually expressed in terms of a limit on the element Courant number. The element Courant number $C_{\Delta t}$ is defined as

$$C_{\Delta t} = \| \mathbf{u} \| \Delta t / h \tag{2.33}$$

3. In the SUPG formulation the choice of

$$\tau = \alpha \Delta t \tag{2.34}$$

leads to a symmetric positive-definite $\mathbf{M}^*$ for purely hyperbolic problems.

Proof:

Consider the following semi-discrete (spatially continuous) formulation of (2.1):

$$(\Phi_{n+1} - \Phi_n) / \Delta t = \mathbf{u} \cdot \nabla \left((1-\alpha) \Phi_n + \alpha \Phi_{n+1} \right) \tag{2.35}$$

For the weak form of (2.35) we employ a weighting function $\tilde{w}$ which is given as

$$\tilde{w} = w + \tau \, \mathbf{u} \cdot \nabla w \tag{2.36}$$

where w and Φ come from the same space. Note that for this purely hyperbolic system a Dirichelet type boundary condition for Φ is required on the part of the boundary where the information comes from outside the domain, and w has to satisfy the homogeneous form at the same boundary condition. That is

$$\Phi(\mathbf{x}) = g(\mathbf{x}) \qquad \forall \mathbf{x} \in \{ \mathbf{x} \mid \mathbf{x} \in \Gamma, \mathbf{n}(\mathbf{x}) \cdot \mathbf{u}(\mathbf{x}) < 0 \} \tag{2.37}$$

$$w(\mathbf{x}) = 0 \qquad \forall \mathbf{x} \in \{ \mathbf{x} \mid \mathbf{x} \in \Gamma, \mathbf{n}(\mathbf{x}) \cdot \mathbf{u}(\mathbf{x}) < 0 \} \tag{2.38}$$

The weak form of (2.35) with the weighting function of (2.36) can be written as follows:

$$(w, \Phi_{n+1}) + \alpha \Delta t\, (w, \mathbf{u} \cdot \nabla \Phi_{n+1}) + \alpha \Delta t\, (\mathbf{u} \cdot \nabla w, \Phi_{n+1})$$

$$+ (\alpha \Delta t)^2 (\mathbf{u} \cdot \nabla w, \mathbf{u} \cdot \nabla \Phi_{n+1}) = \text{R.H.S.} \tag{2.39}$$

where the bilinear form $(\bullet, \bullet)$ is defined as

$$(w, \Phi) = \int_{\Omega} w \Phi \, d\Omega \tag{2.40}$$

Note that only the L.H.S. of (2.39) corresponds to $\mathbf{M}^*$.
Rewriting (2.39) we get

$$(w + \alpha \Delta t\, \mathbf{u} \cdot \nabla w, \Phi_{n+1} + \alpha \Delta t\, \mathbf{u} \cdot \nabla \Phi_{n+1}) = \text{R.H.S.} \tag{2.41}$$

We need to show that the L.H.S. is a symmetric positive-definite form. It is obvious that this bilinear form is symmetric and that

$$(w + \alpha \Delta t\, \mathbf{u} \cdot \nabla w,\ w + \alpha \Delta t\, \mathbf{u} \cdot \nabla w) \geq 0 \tag{2.42}$$

It also needs to be shown that if

$$(1/\alpha \Delta t)\, w + \mathbf{u} \cdot \nabla w = 0 \tag{2.43}$$

then

$$w = 0 \tag{2.44}$$

Note that (2.43) is nothing more than a linear, steady-state, convection-reaction type equation for w. Since $(1/\alpha \Delta t)$ is always positive, the reaction is a consumption on w. If the value of w at any point can be traced back to a boundary point, because of (2.38) w = 0; if not, w = 0 because of consumption. This completes our proof, based partly on physical reasoning, that $\mathbf{M}^*$ is symmetric positive-definite.

3. Element-by-Element (EBE) Approximate Factorization.

The equation system of (2.28) can be rewritten as follows:

$$\mathbf{A}\,\mathbf{x} = \mathbf{b} \tag{3.1}$$

where $\mathbf{x}$ is the increment vector $\Delta\mathbf{a}$, $\mathbf{b}$ is the residual vector $\mathbf{R}$, and $\mathbf{A}$ is the coefficient matrix $\mathbf{M}^*$.

A parabolic regularization of (3.1) can be expressed as

$$\mathbf{W}\, d\mathbf{y}/d\theta + \mathbf{A}\,\mathbf{y} = \mathbf{b} \tag{3.2}$$

where θ is a dimensionless "pseudo-time" and

$$\mathbf{y}(0) = \mathbf{0} \tag{3.3}$$

We assume that

$$\mathbf{x} = \lim_{\theta \to \infty} \mathbf{y}(\theta) \tag{3.4}$$

The choice of $\mathbf{W}$ depends on the properties of $\mathbf{A}$. For a symmetric positive-definite $\mathbf{A}$ Hughes, Levit and Winget [12,13] proposed $\mathbf{W}$ to be the diagonal part of $\mathbf{A}$; that is

$$\mathbf{W} = \text{diag}\, \mathbf{A} \tag{3.5}$$

This was found to be effective for all problems studied in [12,13]. Alternately $\mathbf{W}$ can be chosen to be the lumped mass matrix mentioned in Section 2. That is

$$\mathbf{W} = \mathbf{M}_L \tag{3.6}$$

This choice was proposed by Hughes, Winget, Levit and Tezduyar [14].

Since we are interested in the steady-state solution of (3.2), we employ a backward difference pseudo-time stepping algorithm. This is summerized below:

$$(\mathbf{W} + \Delta\theta\, \mathbf{A})\, \Delta\mathbf{y}_m = \Delta\theta\, \mathbf{r}_m \tag{3.7}$$

$$\mathbf{r}_m = \mathbf{b} - \mathbf{A}\, \mathbf{y}_m \tag{3.8}$$

$$\mathbf{y}_{m+1} = \mathbf{y}_m + \Delta\mathbf{y}_m \tag{3.9}$$

Equation (3.7) can also be written as

$$\Delta\mathbf{y}_m = \mathbf{D}\, (\mathbf{I} + \mathbf{DAD})^{-1}\, \mathbf{D}\, \mathbf{r}_m \tag{3.10}$$

where $\mathbf{I}$ is the identity matrix and

$$\mathbf{D} = (\mathbf{W}^{-1}\, \Delta\theta)^{1/2} \tag{3.11}$$

Note that (3.11) requires $\mathbf{W}$ to be positive-definite. While the choice of (3.5) does not guarantee this when $\mathbf{M}^*$ is not positive-definite, the alternate choice of (3.6) does. One also needs to note that for problems in fluid mechanics $\mathbf{M}^*$ in general is not symmetric, positive-definite; however, as mentioned in section 2, the choice (2.34) assures that it is.

The two-pass EBE approximation is based on the following expression:

$$(\mathbf{I} + \mathbf{DAD}) \approx \prod_{e=1}^{nel} (\mathbf{I} + 1/2\, \mathbf{DA}^e\mathbf{D}) \times \prod_{e=nel}^{1} (\mathbf{I} + 1/2\, \mathbf{DA}^e\mathbf{D}) \tag{3.12}$$

where nel is the total number of elements in the domain. Clearly, this approximation depends on the element ordering.

We update $\mathbf{y}_{m+1}$ according to the following formula:

$$y_{m+1} = y_m + s\,\Delta y_m \tag{3.13}$$

where s is a search parameter obtained by minimizing $\| r_{m+1} \|^2$ with respect to s; that is

$$s = (A\,\Delta y_m)\cdot r_m / \| A\,\Delta y_m \|^2 \tag{3.14}$$

Remarks:
1. The need for the formation and storage of the global matrix **A** has been eliminated.
2. There is no need to store the element level matrices A^e's; however, if desired, instead of recomputing for each EBE iteration, the element level matrices can be stored. Even then, the storage requirement is far less than that of a global matrix.
3. The EBE approximate factorization procedure is parallelizable.
4. It must be well understood that if the EBE procedure converges, it converges to the solution of (3.1), which is the equation system of the implicit method.

4. Implicit-Explicit Approximation Schemes.

Let $\mathcal{E}$ be the set of all elements, e = 1,2,.....,nel. The assembly of the global matrix **M*** cab be expressed as follows:

$$M^* = \mathop{\mathbf{A}}_{e\in\mathcal{E}} (m^*)^e \tag{4.1}$$

where $\mathbf{A}$ is the assembly operator.

Let $\mathcal{E}_I$ and $\mathcal{E}_E$ be the subsets of $\mathcal{E}$ corresponding to "implicit elements" and "explicit elements" respectively, such that:

$$\mathcal{E} = \mathcal{E}_I \cup \mathcal{E}_E \tag{4.2}$$

$$\varnothing = \mathcal{E}_I \cap \mathcal{E}_E \tag{4.3}$$

Rewriting (4.1) we get

$$M^* = \mathop{\mathbf{A}}_{e\in\mathcal{E}_I} (m^*)^e + \mathop{\mathbf{A}}_{e\in\mathcal{E}_E} (m^*)^e \tag{4.4}$$

Implicit-explicit approximation [15,16] is based on the replacement of $(m^*)^e$ by the element level lumped mass matrix $(m)^e_L$; that is:

$$M^* = \mathop{\mathbf{A}}_{e\in\mathcal{E}_I} (m^*)^e + \mathop{\mathbf{A}}_{e\in\mathcal{E}_E} (m)^e_L \tag{4.5}$$

The selection of the implicit elements is based on the stability criterion which is defined in terms of the estimated element Courant number.

5. Adaptive Implicit-Explicit (AIE) Approximation Schemes.

We propose that the set $\mathcal{E}_I$ and $\mathcal{E}_E$ are determined dynamically. The determination will be based on several criteria including stability considerations for all types of transport penomena present. Stability and accuracy characteristics of algorithms are described not only in terms of the element Courant number but also in terms of the dimensionless wave number (see [19]). Therefore, we believe that in the determination of the implicit elements the dimensionless wave number for the solution from the previous time step (or iteration) should play a significant role. We can achieve this by defining a determination criterion which is also based on some measure of the jump in the solution or jump in the flux across an element under consideration. The jump values are computed based on the previous time step (or iteration). Currently we employ the following definition for the jump in the solution across an element:

$$[\Phi] = \max_a (\Phi_a) - \min_a (\Phi_a) \tag{5.1}$$

where a is the element node number. Note that the threshold value for this jump which makes the element eligible for the implicit set $\mathcal{E}_I$ should be based on the global scaling of
the solution field. Such a global scaling idea is closely related to the global scaling concept of the "discontinuity capturing" scheme described in [20].

In the AIE approach one can have a high degree of refinement throughout the mesh but can raise the implicit flag only for those elements which are proposed to be treated implicitly.

Compared to other adaptive concepts such as adaptively moving grids or adaptive element-subdividing the AIE scheme is far easier to implement because it involves no geometric changes; the bookkeeping involved is minimal.

6. Numerical Examples.

The EBE, implicit-explicit, and AIE schemes have been tested on various problems governed by the model equations stated in section 2. The results are compared with those obtained from the implicit and explicit schemes.

two-dimensional advection of a cosine hill (translating puff).

This problem consists of advection of a cosine hill from the extreme left to the right. Two meshes are tested: a uniform mesh with 30×30 elements in a 1×1 domain and a nonuniform mesh with 45×30 elements in a 1×0.75 domain.

For the uniform mesh an initial cosine hill profile with unit peak amplitude and base radius of 0.2 is centered at $(x_1,x_2) = (0.267, 0.5)$. The diffusion coefficient is set to be 10^{-6}; the advection velocity is unity in x_1-direction, and the time step is adjusted to give a Courant number of 0.6. Homogeneous Dirichelet boundary condition is specified on all boundaries except at $x_1 = 1.0$ where homogeneous Neumann boundary condition is imposed. Figures 1(a)-1(c) show the results at various times obtained by one pass AIE scheme (AIE-1). Figures 2(a)-2(c) show the distribution of the implicit elements at the corresponding times for the AIE-1 computations. Implicit, EBE, and explicit one pass (EXP-1) schemes are also tested.The peak amplitude value of the cosine hill at $t = 0.72$ is: 0.972 for the implicit and EBE schemes, and 0.974 for AIE-1. EXP-1 gives a stable solution with poor accuracy.

For the nonuniform mesh the element length in the left region of the domain is half of that in the right region. Time step is chosen such that the Courant number is 1.8 in the left and 0.9 in the right. The initial profile is centered at $(x_1,x_2) = (0.233, 0.375)$

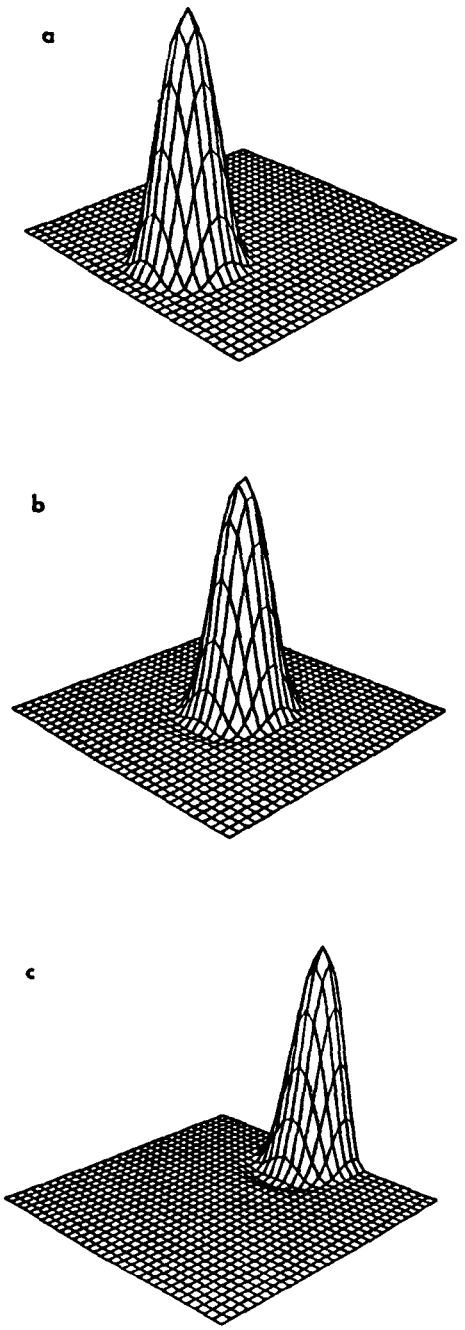

Fig. 1. Elevation plots for the translating puff obtained by the AIE-1 scheme. (a) Initial condition. (b) at t = 0.3 . (c) at t = 0.72 .

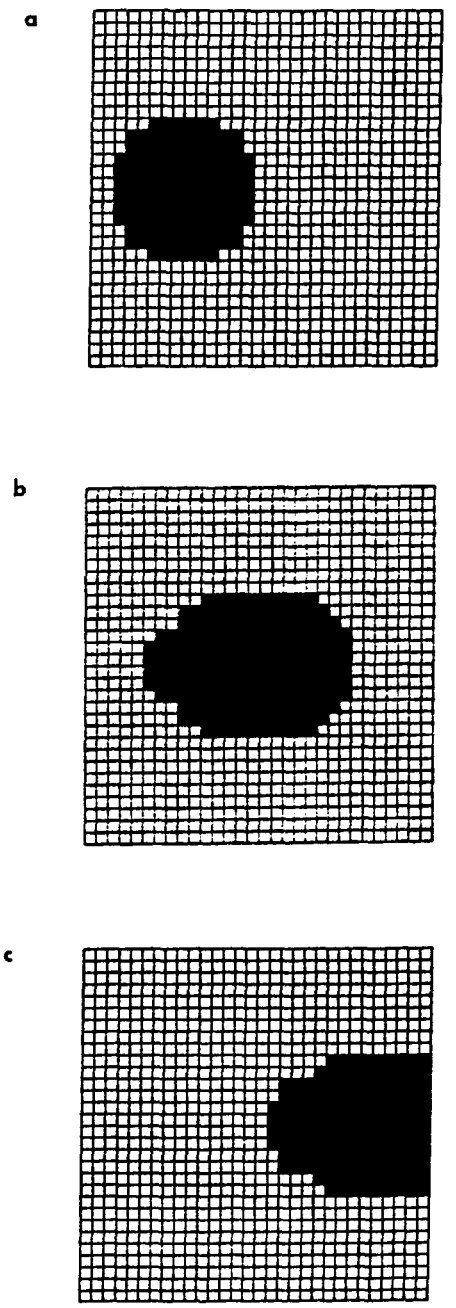

Fig. 2. Distribution of the implicit elements for the AIE calculations of the translating puff. (a) at t = 0 . (b) at t = 0.3. (c) at t = 0.72 .

with base radius of 0.2. All other set-up conditions are the same as in the case of the uniform mesh. Figures 3(a)-3(c) show the elevation plots at various times obtained by the two pass implicit-explicit scheme (IMEX-2). Figure 4(a) shows the distribution of the implicit elements. The peak amplitude value at t = 0.72 is: 0.969 for the implicit and EBE schemes, 0.985 for IMEX-2. The results for the explicit two pass (EXP-2) scheme are shown in Figures 4(b)-4(c). It can be seen in Figure 4(c) that in the left region of the domain the solution becomes unstable due to the high Courant number.

The mean bandwidth (averaged over the number of time steps) of the global coefficient matrix for the AIE scheme in the case of the unifrom mesh is 25% of that for the implicit scheme. The average number of implicit elements at each time step is 173. For the nonuniform mesh the mean bandwidth for the IMEX scheme is 78%, and the number of implicit elements is 1016.

two-dimensional rigid body rotation of a cosine hill (rotating puff).

The set-up conditions for this problem are the same as in the uniform mesh case of the translating puff problem except that the velocity field is rotational with respect to the center of the domain. (i.e. $u_1 = - x_2 + 0.5$, $u_2 = x_1 - 0.5$), and all boundary conditions are Dirichelet type and homogeneous. The time step is adjusted to give a Courant number of 0.216 at the tip of the cosine hill. A full revolution is achieved in 200 time steps. Figures 5(a)-5(c) show the results at various times obtained by AIE-1. Figures 6(a)-6(c) show the distribution of the implicit elements at the corresponding times. The peak amplitude after a full revolution is found to be 0.984 for the implicit and EBE schemes, and 0.980 for AIE-1. The mean bandwidth (averaged over the number of time steps) for the AIE scheme is 26% of the implicit scheme. The average number of implicit elements at each time step is 173. As in the case of the translating puff (uniform mesh), the results for EXP-1 are not satisfactory. Figures 7(a)-7(b) and Figures 8(a)-8(b) demonstrate the performance of EXP-1 in both cases.

flow past a circular cylinder.

In this problem we have 1940 elements and 2037 nodal points. A refined and implicit zone is located around the cylinder. Diffusivity is 0.0025 giving a Reynolds number of 100 based on the diameter of the cylinder. The time step is fixed at 1.0. The number of corrections at each time step is allowed to be as many as the convergence criterion (10^{-6}) dictates.The mesh, the boundary conditions, and the distribution of the implicit elements are shown in figure 9(a). Figures 9(b)-9(c) show the streamlines and isovorticity lines for the symmetric solution at time = 400 obtained by the EBE scheme. After that, an artificial disturbance is placed shortly to initiate a nonsymmetric solution. Figures 10(a)-10(c) show the nonsymmetric results at time = 1,200 for the EBE scheme. The implicit, EBE , and the implicit-explicit schemes all give very close results (differences less than 0.5%). The explicit scheme diverges. The mean bandwidth of the implicit-explicit scheme is 47% of the implicit scheme. The number of implicit elements is 320.

driven cavity flow.

A uniform mesh of 30 × 30 elements in a 1 × 1 domain is chosen. Diffusivity is 0.0025, time step is 0.1, and Reynolds number is 400 based on the side length of the square domain. The number of corrections at each time step is limited to 5. Figure 11(a) shows the mesh, the boundary conditions, and the distribution of the implicit elements. Results obtained by the implicit-explicit scheme are shown in Figures 11(b)-11(d). These results are indistinguishable from those obtained by the implicit and EBE schemes (differences less than 0.001%). The mean bandwidth for implicit-explicit

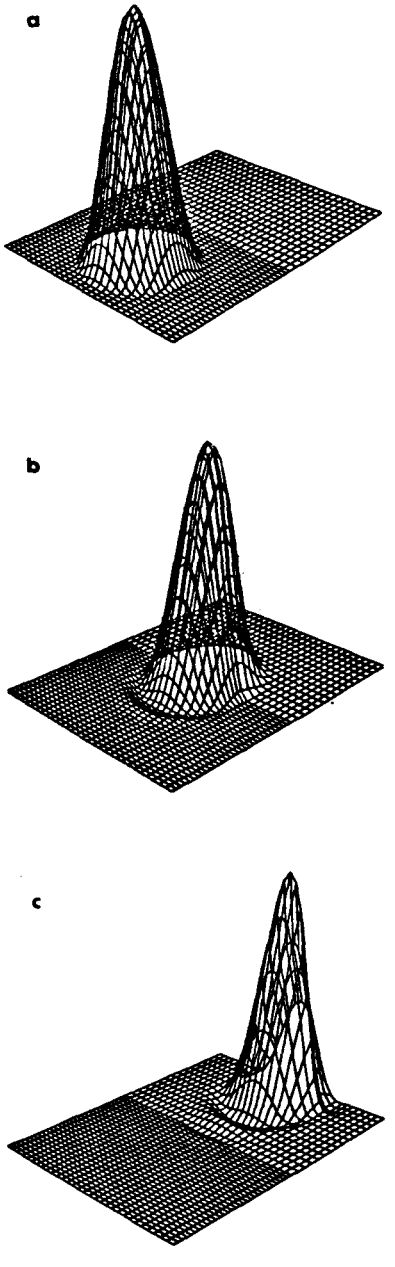

Fig. 3. Translating puff problem on a nonuniform mesh. Results obtained by the IMEX-2 scheme. (a) Initial condition. (b) at t=0.3. (c) at t=0.72.

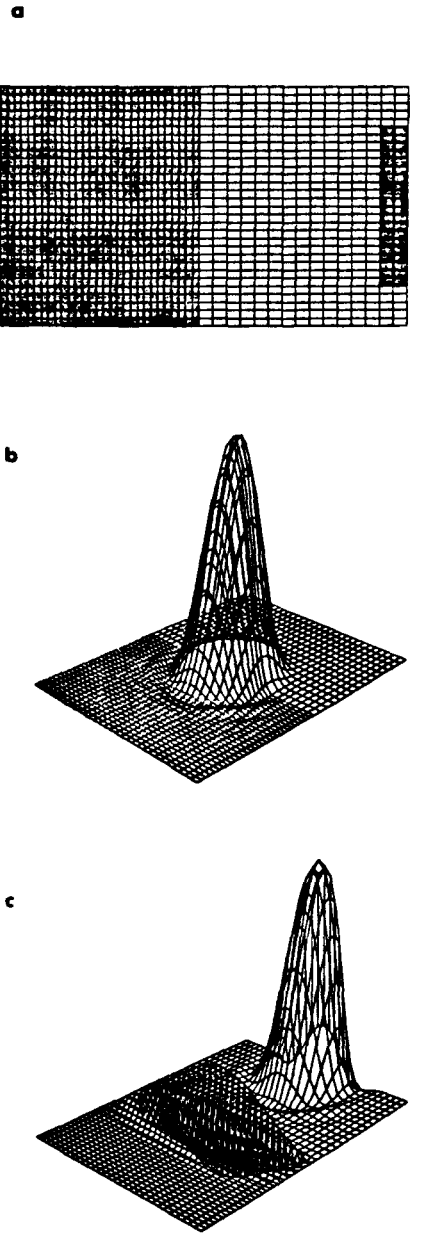

Fig. 4. Translating puff problem on a nonuniform mesh. (a) Distribution of the implicit elements for the IMEX scheme. (b) and (c) Results obtained by the EXP-2 scheme at t = 0.3 and t = 0.72 .

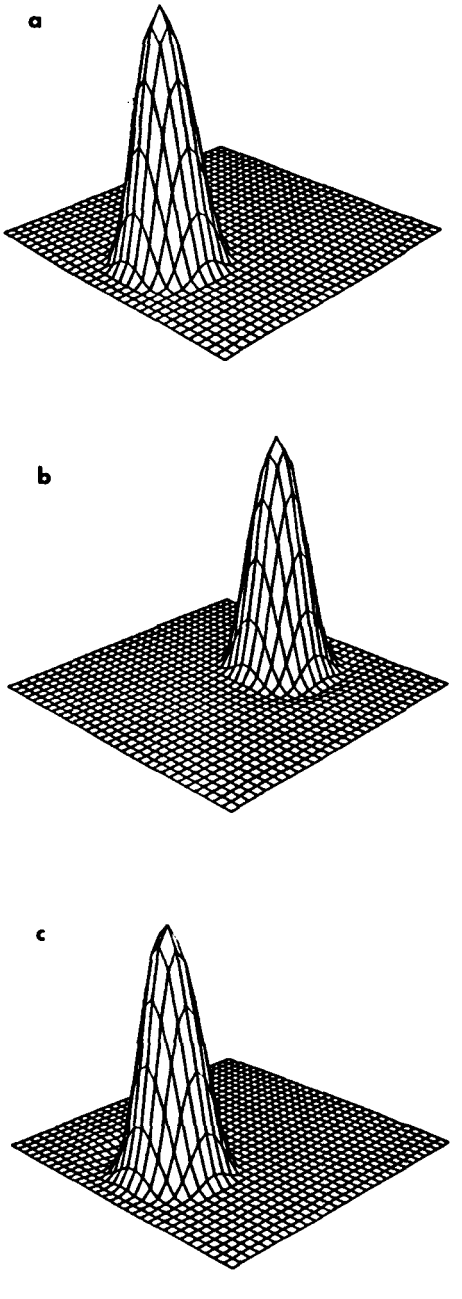

Fig. 5. Elevation plots for the rotating puff obtained by the AIE-1 scheme. (a) Initial condition. (b) at t = 3.14 . (c) at t = 6.28.

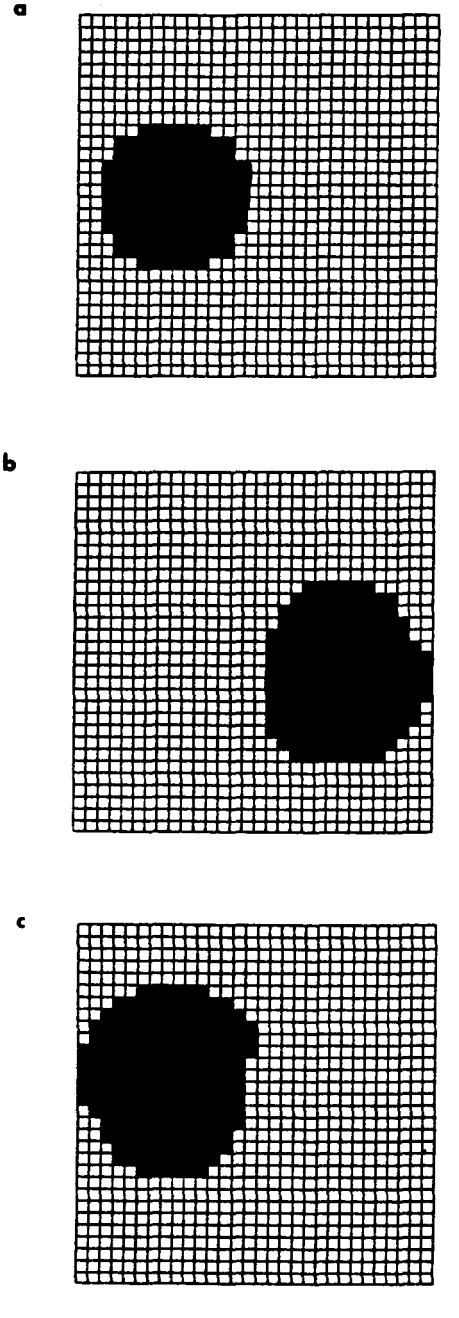

Fig. 6. Distribution of the implicit elements for the AIE calculations of the rotating puff. (a) at t = 0 . (b) at t = 3.14. (c) at t = 6.28 .

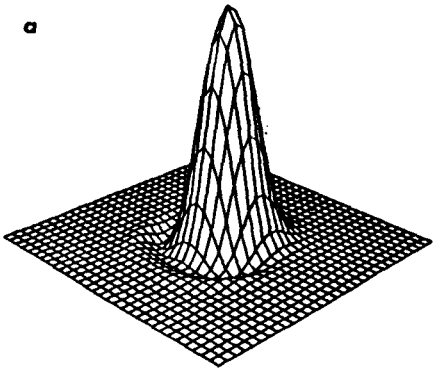

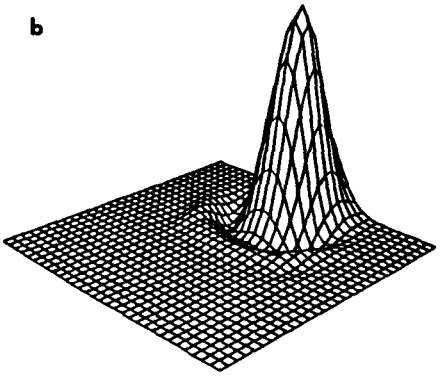

Fig. 7. Elevation plots for the translating puff obtained by the EXP-1 scheme on a uniform mesh. (a) at $t = 0.3$. (b) at $t = 0.72$.

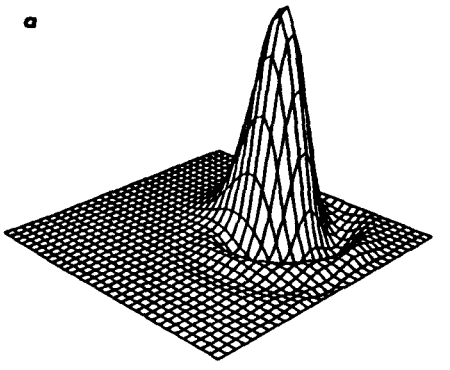

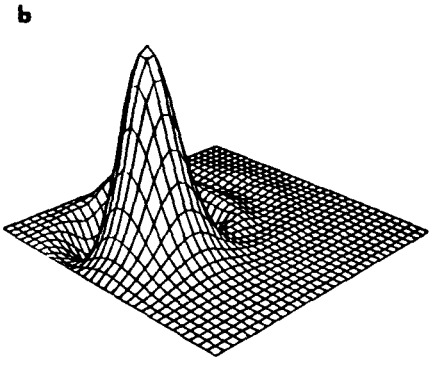

Fig. 8. Elevation plots for the rotating puff obtained by the EXP-1 scheme on a uniform mesh. (a) at $t = 3.14$. (b) at $t = 6.28$.

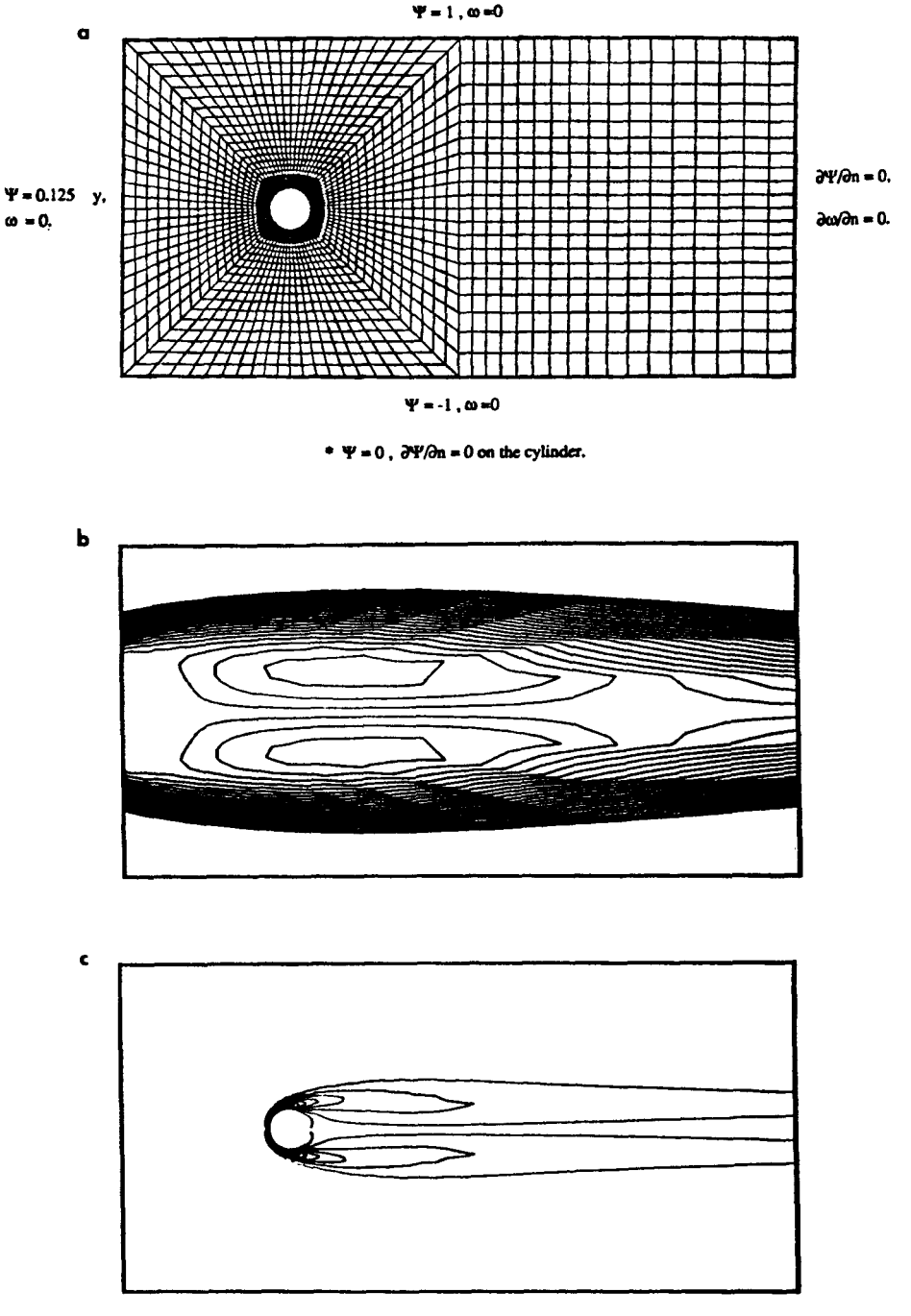

Fig. 9. Flow past a circular cylinder at Reynolds number 100. Symmetric solutions. (a) Finite element mesh, boundary conditions and the distribution of the implicit elements for the IMEX calculations. (b) Local streamlines obtained by the EBE scheme at t = 400. (c) Iso-vorticity lines obtained by the EBE scheme at t = 400 .

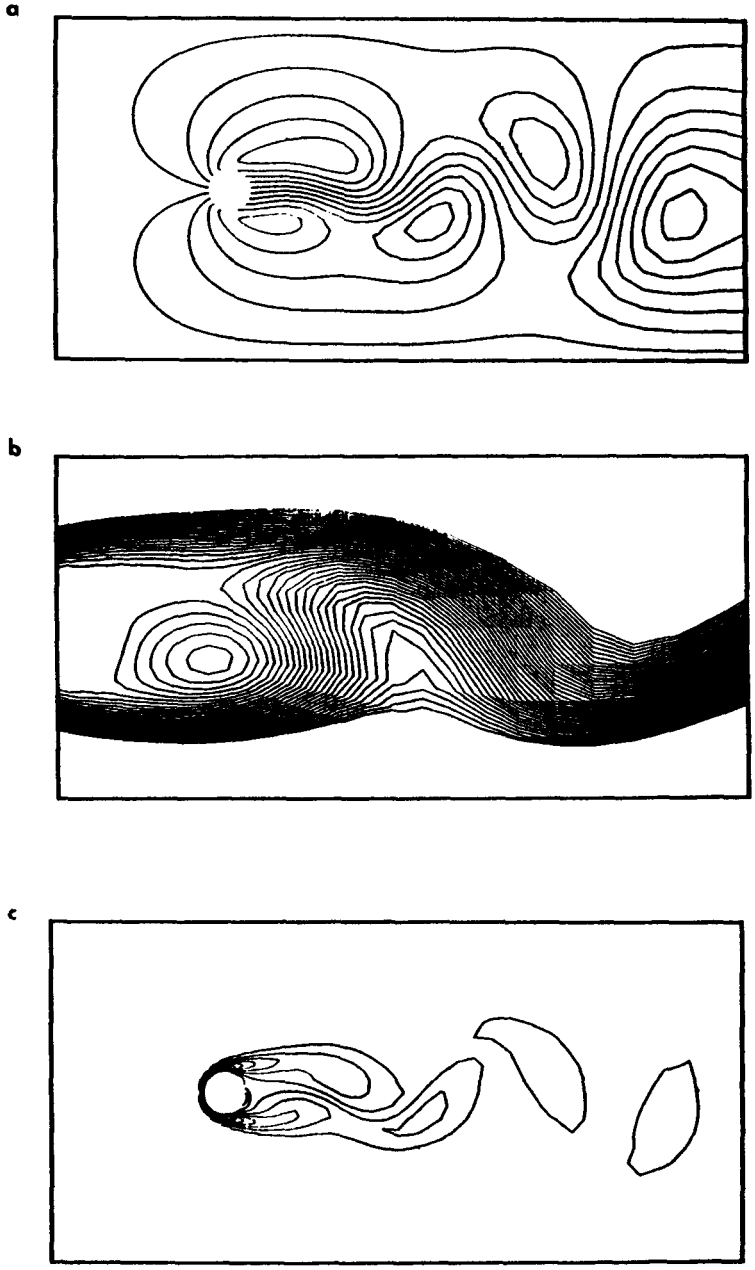

Fig. 10. Flow past a circular cylinder at Reynolds number 100. Nonsymmetric solutions obtained by the EBE scheme at $t = 1200$. (a) Relative streamlines. (b) Local streamlines. (c) Iso-vorticity lines.

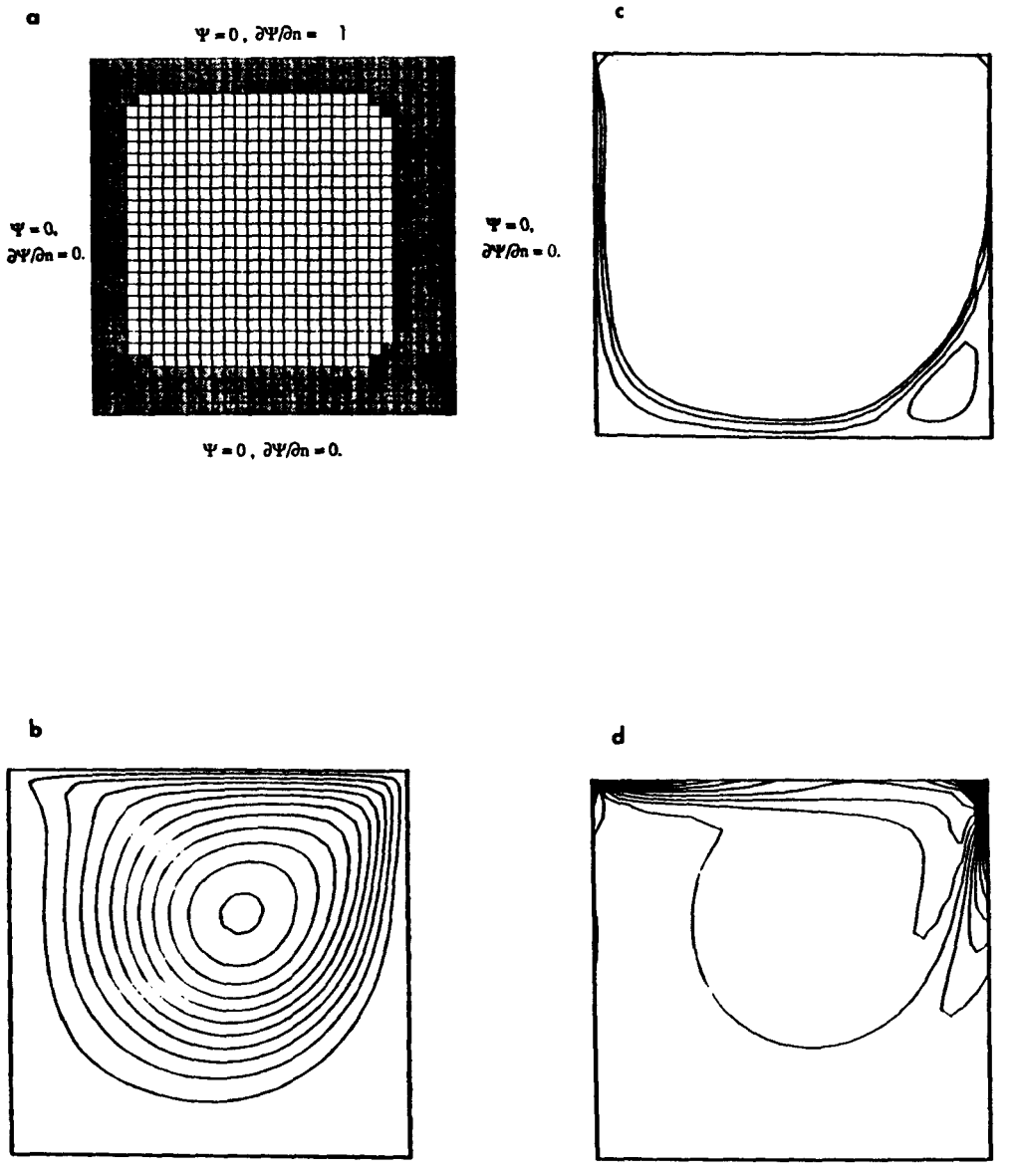

Fig. 11. Driven cavity flow at Reynolds number 400. Solutions obtained by the IMEX scheme at t = 10. (a) Finite Element mesh, boundary conditions and the distribution of the implicit elements. (b) Streamlines. (c) Corner streamlines. (d) Iso-vorticity lines.

scheme is 44% of the implicit scheme.The number of implicit elements is 403.

7. Conclusions.

In this paper we have presented approximate solution schemes for large equation systems resulting from finite element formulation of fluid dynamics problems. The element-by-element (EBE) approximate factorization scheme is essentially an iterative scheme which totally eliminates the need for the formation, storage, and inversion of a large global matrix. Implicit-explicit schemes in nature are approximations to implicit schemes, yet they substantially reduce the cost of formation, storage, and inversion of a large global matrix. In the adaptive implicit-explicit (AIE) scheme, the implicit elements are selected adaptively based on local stability and accuracy conditions. This scheme allows us to have implicit refinement where it is needed.

We have applied these schemes to various problems governed by the convection-diffusion equation and the vorticity-stream function form of the two-dimensional Navier-Stokes equations. The results in all cases are indistinguishable from those obtained by true implicit formulations. We are convinced that it will not be very long before these schemes are accepted as powerful tools in large-scale computing.

REFERENCES

[1] R. Glowinski, Q.V. Dinh, and J. Periaux, Domain Decomposition Methods for Nonlinear Problems in Fluid Dynamics, Computer Methods in Applied Mechanics and Engineering, 40 (1983), pp. 27-109.

[2] C.C. Paige and M.A. Saunders, LSQR: An Algorithm for Sparse Linear Equations and Sparse Least Square, ACM Transactions on Mathematical Software, 8 (1982), pp. 43-71.

[3] G.W. Stewart, Conjugate Direction Methods for Solving Systems of Linear Equations, Numer. Math., 21 (1973), pp. 285-297.

[4] D.M. Young, Second-Degree Iterative Methods for the Solution of Large Linear Systems, J. Approx. Theory, 5 (1972), pp. 137-148.

[5] R. S. Rogallo, Numerical Experiments in Homogeneous Turbulence, NASA TN 81315, September 1981.

[6] D. Heller, A Survey of Parallel Algorithms in Numerical Linear Algebra, SIAM Review, 20 (1978), pp. 740-777.

[7] J.M. Frailong and J. Pakleza, Resolution of General Partial Differential Equations on a Fixed Size SIMD/MIMD Large Celluar Processor, in Proceedings of the IMACS International Congress, Sorente, Italie, (Sept. 1979).

[8] R. Glowinski, Numerical Methods for Nonlinear Variational Problems, Springer-Verlag, New York, 1984.

[9] D.W. Peaceman and H. H. Rachford, The Numerical Solution of Parabolic and Elliptic Differential Equations, J. Soc. Indust. Appl. Math, 3 (1955), pp. 28-41.

[10] J. Douglas, H.H. Rachford,On the Numerical Solution of Heat Conduction Problems in Two and Three Space Variables, Trans. Am. Math. Soc. , 82 (1956), pp. 421-439.

[11] N.N. Yanenko, The Method of Fractional Steps, Springer-Verlag, New York, 1971.

[12] T. J. R. Hughes, I. Levit and J. Winget, Element-By-Element Implicit Algorithms for Heat Conduction, Journal of the Engineering Mechanics Division, ASCE, 109 (1983), pp. 576-585.

[13] T. J. R. Hughes, I. Levit and J. Winget, An Element-by-Element Solution Algorithm for Problems of Structural and Solid Mechanics, Computer Methods in Applied Mechanics and Engineering, 36 (1983), pp. 241-254.

[14] T.J.R. Hughes, J. Winget, I. Levit, T.E. Tezduyar, New Alternating Direction Procedures in Finite Element Analysis Based upon EBE Approximate Factorizations, in Computer Methods for Nonlinear Solids and Mechanics, S. N. Atluri and N. Perrone, eds., AMD Vol. 54, ASME, New York, 1983, pp.75-110.

[15] T.J.R. Hughes and W.K. Liu, "Implicit-Explicit Finite Elements in Transient Analysis: Stability Theory," Journal of Applied Mechanics, 45 (1978), pp. 371-374.

[16] T.J.R. Hughes and W.K. Liu, Implicit-Explicit Finite Elements in Transient Analysis: Implementation and Numerical Examples, Journal of Applied Mechanics, 45 (1978), pp. 375-378.

[17] T.E. Tezduyar and D.K. Ganjoo, Petrov-Galerkin Formulations with Weighting Functions Dependent upon Spatial and Temporal Discretization: Applications to Transient Convection-Diffusion Problems, Computer Methods in Applied Mechanics and Engineering, 59 (1986), pp. 47-71.

[18] T.J.R. Hughes, Analysis of Transient Algorithms with particular Reference to Stability Behavior, Computational Methods for Trnasient Analysis, Ted Belytschko and T.J.R. Hughes, eds., North Holland Publishing Co., Amsterdam, 1984.

[19] T.E. Tezduyar and T.J.R. Hughes, Development of Time-accurate Finite Element Techniques for First-order Hyperbolic System with Particular Emphasis on the Compressible Euler Equations, Final Report, NASA-Ames University Consortium Interchange No. NCA2-OR745-104, April 1982.

[20] T.E. Tezduyar and Y.J. Park, Discontinuity-Capturing Finite Element Formulations for Nonlinear Convection-Diffusion-Reaction Equations, Computer Methods in Applied Mechanics and Engineering 59 (1986), pp.307-325.